Int. J. Heat Mass Transfer. Vol. 26, No. 3, pp. 433–444, 1983
Printed in Great Britain

0017 9310/83/030433 12 $03.00/0

MIXED CONVECTION PLUME ABOVE A HORIZONTAL LINE SOURCE SITUATED IN A FORCED CONVECTION APPROACH FLOW

S. E. HAALAND* and E. M. SPARROW
Department of Mechanical Engineering, University of Minnesota, Minneapolis, MN 55455, U.S.A.

(*Received* 12 *May* 1982 *and in revised form* 29 *July* 1982)

Abstract—Both analytical and numerical techniques were employed to solve for the velocity and temperature fields in a two-dimensional mixed convection plume for the Prandtl number range from 0.72 to infinity. The method of inner and outer expansions was used for the $Pr = \infty$ case while a parabolic, finite-difference method yielded the solutions for the other Prandtl numbers. In general, the plume was found to evolve with increasing distance from the line source from one with a basically forced convection character to one which resembles that for pure natural convection. The centerline velocity and temperature variations with distance from the line source were bounded by envelope curves constructed from the asymptotes for pure forced and pure natural convection. Highly accurate algebraic relations valid for all Prandtl numbers and all distances above the line source were developed to generalize the results obtained for the various discrete Prandtl numbers. The plume width increased with distance from the source, but at a slower rate at greater distances. The shapes of the velocity profiles changed both with distance and Prandtl number, whereas all temperature profiles displayed a common bell-like shape.

NOMENCLATURE

A, x-portion of $\tilde{T}$, equation (26);
a, constant, equal to 1.0;
a_0, b, constant, equal to $F'(0)$;
B, x-portion of ψ, equation (40);
cn constant, equal to 0.282;
c_p, specific heat;
d, constant, equal to $H(0)/Pr^{1/2}$;
F, velocity similarity variable, equation (A6);
G, gravitational acceleration group, $g\beta Q/\rho c_p \nu$;
Gr, Grashof number, $g\beta\theta_T \bar{x}^3/\nu^2$;
g, acceleration of gravity;
H, temperature similarity variable, equation (A7);
h, natural convection plume width scale, equation (A8);
h_∞, plume width scale, equation (26);
K, ζ-portion of ψ, equation (40);
L, characteristic length, $\bar{u}_\infty^5/[\nu(g\beta\theta_T)^2]$;
m, exponent in equation (54);
N, $\tilde{\eta}$-portion of $\tilde{T}$, equation (26);
n, exponent in equation (52);
Pr, Prandtl number;
Q, rate of heat input at line source;
R, Reynolds number, $(\bar{u}_\infty L/\nu)^{1/2}$;
Re, Reynolds number, $\bar{u}_\infty \bar{x}/\nu$;
T, dimensionless temperature, equation (7a);
$\bar{T}$, temperature;
u, v, dimensionless velocities, equation (7a);
$\bar{u}, \bar{v}$, velocity components;
x, y, dimensionless coordinates, equation (7b);
$\bar{x}, \bar{y}$, coordinates.

Greek symbols

β, coefficient of thermal expansion;
δ, dimensionless velocity profile half-width;
δ_T, dimensionless temperature profile half-width;
ζ, similarity variable, equation (41);
η, similarity variable, equation (A8);
$\tilde{\eta}$, similarity variable, equation (26);
θ_T, a characteristic temperature, $Q/\rho c_p \nu$;
ν, kinematic viscosity;
ρ, density;
ψ, dimensionless stream function, $\bar{\psi} R/\bar{u}_\infty L$;
$\bar{\psi}$, stream function;
ω, transverse coordinate for numerical computation, $\bar{\psi}/\bar{\psi}_e$.

Subscripts

e, edge of boundary layer;
0, centerline;
∞, free stream.

Superscripts

$\tilde{}$, inner region variable;
$\bar{}$, dimensional quantity.

1. INTRODUCTION

THE MIXED convection plume due to a horizontal line source of heat (or mass) situated in a uniform vertical flow is of interest in several engineering applications. These include, for example, hot-wire and hot-film anemometry, thermal pollution, and dispersion of pollutants (i.e. dispersion of mass). Furthermore, these applications may encompass heat or mass transfer in a

* On leave from The Norwegian Institute of Technology, N-7034, Trondheim-NTH, Norway.

variety of fluids, so that the relevant range of the Prandtl or Schmidt number may extend from about 0.7 to several thousand. The objective of this investigation is to obtain information about the plume velocity and temperature fields over the range $0.72 \leqslant Pr \leqslant \infty$.

The physical processes which occur in the plume are such that, at very high Prandtl numbers, the velocity field is very much broader than the temperature field. For this situation, it is advantageous to obtain solutions by employing the method of inner and outer expansions. This method was used in the paper to solve the $Pr = \infty$ case. In this connection, it is well established that for natural convection boundary layer flows, solutions for $Pr = \infty$ provide accurate results for a wide range of finite Prandtl numbers. Solutions for other Prandtl numbers were obtained numerically by a parabolic, fully implicit, finite-difference method.

Algebraic generalizations of the results for the centerline velocity and temperature variations with vertical distance from the line source were developed. These algebraic representations yield highly accurate results for all Prandtl numbers in the investigated range and for all vertical distances. The graphical presentation of results encompassed the centerline velocity and temperature distributions, the velocity and thermal widths of the plume, and representative velocity and temperature profiles.

In considering the available literature, it is relevant to note that a mixed convection plume undergoes an evolution with increasing vertical distance from the line source. The evolution starts with a near-field flow where forced convection is dominant, passes through a regime where buoyancy and forced convection are of comparable magnitude, and finally emerges as a far-field flow where natural convection is dominant. The near-field flow (i.e. a weakly buoyant plume) has been studied [1–3]. Of these, ref. [3] also considered the far-field flow. A complete solution of the mixed convection problem has been given for a Prandtl number of 0.72 [4].

Afzal [4] solved the problem in terms of two coordinate expansions: a direct coordinate expansion for a weakly buoyant plume (i.e. applicable to the near field), and an inverse coordinate expansion for a strongly buoyant plume (i.e. applicable to the far field). It was shown, however, that if the series for the weakly buoyant plume is suitably transformed, it can describe very accurately the solution in the entire domain of the flow. Afzal's solution method, even though of considerable interest due to the use of sophisticated techniques for series manipulation to improve the accuracy, still requires a considerable amount of numerical work to find the solution of a large number of interrelated ordinary differential equations. In fact, the amount of required numerical work may well exceed that needed for a direct numerical solution of the problem.

Numerical solutions in the limit $Pr \to \infty$ for the pure natural convection case have been obtained by Spalding and Cruddace [5] and by Kuiken and Rotem [6]. For forced convection dominant flows, analytical series solutions are available [4], which show the Prandtl number dependence. However, the limit as $Pr \to \infty$ does not appear to have been worked out for the mixed convection plume.

In the presentation that follows, the governing equations are first formulated in general, after which the high Prandtl number solution is developed (including a closed-form, near-field solution). This is followed by a description of the numerical finite difference method. The results are then presented and discussed and, finally, the key findings are summarized.

2. GOVERNING EQUATIONS

Let us consider the mixed-convection plume above a 2-dim. horizontal line source of heat situated in a vertical stream that approaches the line source from below with a uniform velocity. The boundary layer equations for this flow, using the Boussinesq approximation, are

$$\frac{\partial \bar{u}}{\partial \bar{x}} + \frac{\partial \bar{v}}{\partial \bar{y}} = 0, \tag{1}$$

$$\bar{u}\frac{\partial \bar{u}}{\partial \bar{x}} + \bar{v}\frac{\partial \bar{u}}{\partial \bar{y}} = \nu\frac{\partial^2 \bar{u}}{\partial \bar{y}^2} + g\beta(\bar{T} - \bar{T}_\infty), \tag{2}$$

$$\bar{u}\frac{\partial \bar{T}}{\partial \bar{x}} + \bar{v}\frac{\partial \bar{T}}{\partial \bar{y}} = \frac{\nu}{Pr}\frac{\partial^2 \bar{T}}{\partial \bar{y}^2}. \tag{3}$$

Here, $\bar{x}$ is the vertical coordinate and $\bar{y}$ is normal to it. The line source is situated at the origin of coordinates, $\bar{x} = \bar{y} = 0$. (The $\bar{z}$ coordinate is horizontal and lies along the line source.) The velocity and temperature distributions must be symmetrical with respect to the vertical axis, and they must take on the free-stream values outside the plume. Thus, we have the following boundary conditions:

$$\bar{y} = 0, \quad \bar{v} = \partial \bar{u}/\partial \bar{y} = \partial \bar{T}/\partial \bar{y} = 0, \tag{4}$$

$$\bar{y} = \infty, \quad \bar{u} = \bar{u}_\infty, \quad \bar{T} = \bar{T}_\infty \tag{5}$$

In addition, an integral condition can be derived which relates the dependent variables to the constant rate of heat input Q at the line source. First, the energy equation (3) is integrated with respect to $\bar{y}$ to yield, after use of equations (4) and (5),

$$\frac{\mathrm{d}}{\mathrm{d}\bar{x}}\int_{-\infty}^{\infty} \bar{u}(\bar{T} - \bar{T}_\infty)\,\mathrm{d}\bar{y} = 0.$$

This expresses the fact that since there are no sources or sinks of energy anywhere in the flow for $\bar{x} > 0$, the energy transported through each plane $\bar{x}$ = constant is a constant which must be equal to the rate at which energy is released by the source, Q, at $\bar{x} = 0$. Therefore,

$$Q = \rho c_p \int_{-\infty}^{\infty} \bar{u}(\bar{T} - \bar{T}_\infty)\,\mathrm{d}\bar{y}. \tag{6}$$

The governing equations are made non-dimensional by introducing dimensionless variables defined by

$$\bar{u} = \bar{u}_\infty u, \quad \bar{v} = \bar{u}_\infty v/R, \quad \bar{T} - \bar{T}_\infty = (\theta_T/R)T, \tag{7a}$$

$$\bar{x} = Lx, \quad \bar{y} = Ly/R, \quad R = (\bar{u}_\infty L/\nu)^{1/2}, \tag{7b}$$

$$\theta_T = Q/(\rho c_p \nu), \quad L = \bar{u}_\infty^5/[\nu(g\beta\theta_T)^2]. \tag{7c}$$

The respective choices of θ_T/R and L as the characteristic temperature and length, as given by equations (7), were motivated by the fact that they render, respectively, the integral condition (6) and the momentum equation (2) free of parameters. We may note that the present choice of L is possible only because there is no physical length scale in the problem. By substituting equations (7) into equations (1)–(6), we obtain

$$\frac{\partial u}{\partial x} + \frac{\partial v}{\partial y} = 0, \tag{8}$$

$$u\frac{\partial u}{\partial x} + v\frac{\partial u}{\partial y} = \frac{\partial^2 u}{\partial y^2} + T, \tag{9}$$

$$u\frac{\partial T}{\partial x} + v\frac{\partial T}{\partial y} = \frac{1}{Pr}\frac{\partial^2 T}{\partial y^2}, \tag{10}$$

$$y = 0, \quad v = \partial u/\partial y = \partial T/\partial y = 0, \tag{11}$$

$$y = \infty, \quad u = 1, \quad T = 0, \tag{12}$$

$$x \geqslant 0, \quad \int_0^\infty uT\,\mathrm{d}y = 1/2. \tag{13}$$

We may also note that the dimensionless streamwise coordinate x is related to the Reynolds number $Re = \bar{u}_\infty \bar{x}/\nu$ and the Grashof number $Gr = g\beta\theta_T \bar{x}^3/\nu^2$ in the following manner:

$$x = \bar{x}/L = Gr^2/Re^5. \tag{14}$$

The solutions of the system equations (8)–(13) for very small x (pure forced convection) and very large x (pure natural convection) are well known. Therefore, they need not be derived in detail. They will, however, be stated in the Appendix because they serve as limits for the present mixed convection solution. A complete solution for arbitrary x will be found by a finite difference technique as will be described in Section 4; but first, in the next section, we will study the limit as $Pr \to \infty$. Previous experience with natural convection boundary layers has shown that the $Pr \to \infty$ solution applies with good accuracy for a wide range of finite Prandtl numbers.

3. HIGH PRANDTL NUMBER LIMIT

For high Prandtl numbers, we can divide the region of interest into two layers, (i) the inner region (adjacent to the symmetry axis) where $T \neq 0$ and (ii) the outer region where $T = 0$. It is known that as the Prandtl number increases the inner region gets increasingly narrow, and in the limit $Pr \to \infty$, the thickness of this layer becomes zero.

3.1. *Inner region*

We introduce stretched variables as follows:

$$\tilde{y} = Pr^{1/2}y, \quad \tilde{v} = Pr^{1/2}v, \quad \tilde{T} = Pr^{-1/2}T. \tag{15}$$

The stretching of y renders the width of the inner layer of order unity. Insertion of equations (15) into equations (8)–(10) and (13) gives

$$\frac{\partial u}{\partial x} + \frac{\partial \tilde{v}}{\partial \tilde{y}} = 0, \tag{16}$$

$$\frac{1}{Pr}\left[u\frac{\partial u}{\partial x} + \tilde{v}\frac{\partial u}{\partial \tilde{y}}\right] = \frac{\partial^2 u}{\partial \tilde{y}^2} + Pr^{-1/2}\tilde{T}, \tag{17}$$

$$u\frac{\partial \tilde{T}}{\partial x} + \tilde{v}\frac{\partial \tilde{T}}{\partial \tilde{y}} = \frac{\partial^2 \tilde{T}}{\partial \tilde{y}^2}, \tag{18}$$

$$1/2 = \int_0^\infty u\tilde{T}\,\mathrm{d}\tilde{y}. \tag{19}$$

Letting $Pr \to \infty$, equation (17) becomes, to zeroth order,

$$\partial^2 u/\partial \tilde{y}^2 = 0. \tag{20}$$

The solution of equation (20) satisfying $\partial u/\partial \tilde{y}(0) = 0$ is

$$u = u_0(x). \tag{21}$$

This says that the velocity must be uniform across the inner layer; in particular, u_0 can be identified as the centerline velocity. However, $u_0(x)$ cannot be determined before the solution for the outer layer has been obtained. With equations (21) and (11), the continuity equation (16) then gives

$$\tilde{v} = -\tilde{y}(\mathrm{d}u_0/\mathrm{d}x) \tag{22}$$

and equation (18) becomes

$$u_0\frac{\partial \tilde{T}}{\partial x} - \tilde{y}\frac{\mathrm{d}u_0}{\mathrm{d}x}\frac{\partial \tilde{T}}{\partial \tilde{y}} = \frac{\partial^2 \tilde{T}}{\partial \tilde{y}^2} \tag{23}$$

with the boundary conditions

$$\tilde{y} = 0, \quad \partial \tilde{T}/\partial \tilde{y} = 0; \quad \tilde{y} = \infty, \quad \tilde{T} = 0. \tag{24}$$

Finally, equation (19) becomes

$$\int_0^\infty \tilde{T}\,\mathrm{d}\tilde{y} = 1/(2u_0). \tag{25}$$

If it is supposed that u_0 were known, one can find a similarity solution for $\tilde{T}$. First, similarity variables are defined as

$$\tilde{T} = A(x)N(\tilde{\eta}), \quad \tilde{\eta} = \tilde{y}/h_\infty(x) \tag{26}$$

where A and h_∞ are, respectively, the scales of temperature and layer thickness. Then, by substituting these variables into the partial differential equation (23), requiring that it reduce to an ordinary differential equation, and using the integral condition (25), there follows

$$h_\infty(x) = 2\left[\int_0^x u_0\,\mathrm{d}x\right]^{1/2}\Big/u_0, \tag{27}$$

$$A(x) = 1/(u_0 h_\infty) \tag{28}$$

and

$$N'' + 2(\tilde{\eta}N)' = 0, \tag{29}$$

$$N'(0) = N(\infty) = 0. \tag{30}$$

The solution of equations (29) and (30), which satisfies equation (19), is

$$N = e^{-\tilde{\eta}^2}/(\pi^{1/2}). \tag{31}$$

The complete solution for the temperature, provided that the velocity u_0 is known has, therefore, been found to be

$$\tilde{T} = e^{-\tilde{y}^2/h_\infty^2}/(\pi^{1/2}u_0 h_\infty) \tag{32}$$

where h_∞ is given by equation (27). Let us now turn to the determination of the velocity.

3.2. *Outer region*

Here, $T = 0$ so that the system, equations (8)–(10), reduces to

$$\frac{\partial u}{\partial x} + \frac{\partial v}{\partial y} = 0, \tag{33}$$

$$u\frac{\partial u}{\partial x} + v\frac{\partial u}{\partial y} = \frac{\partial^2 u}{\partial y^2}, \tag{34}$$

with the boundary conditions

$$v(0) = 0, \quad u(\infty) = 1. \tag{35}$$

The boundary condition $\partial u/\partial y(0) = 0$ can no longer be satisfied. A replacement for this lost boundary condition can be found in a manner similar to that of Spalding and Cruddace [5] for the pure natural convection similarity plume. To begin, the leading terms of the inner-region momentum equation (17) (i.e. with terms of order Pr^{-1} omitted) are integrated across the inner layer from 0 to $\tilde{y}_e$ ($\tilde{y}_e$ being the value of $\tilde{y}$ at the edge of the layer) to yield

$$(\partial u/\partial \tilde{y})_{\tilde{y}_e} - (\partial u/\partial \tilde{y})_0 = -Pr^{-1/2}\int_0^{\tilde{y}_e} \tilde{T}\,d\tilde{y}$$

$$= -Pr^{-1/2}/(2u_0) \tag{36}$$

where equation (25) has been employed to obtain the last equality. Using $\partial u/\partial \tilde{y}(0) = 0$, and then changing to outer variables and letting $Pr \to \infty$, one obtains

$$(\partial u/\partial y)_{y=0} = -1/(2u_0) \tag{37}$$

since $y = \tilde{y}/Pr^{1/2} \to 0$. The required matching condition in the present case is simply to recognize that the function $u_0(x)$ defined on the inner region is also the centerline velocity for the outer problem. Equation (37) serves to complete the slate of boundary conditions for the outer velocity distribution. Equation (37) also serves as a forcing term in lieu of the temperature term which has disappeared in the momentum equation (34).

The system, equations (33)–(35) and (37), does not admit a similarity solution, so that a numerical solution must be found, as will be described in Section 4. However, analytical solutions both for the inner and the outer regions can be found for small x. These will now be derived.

3.3. *Solutions for small x*

For the inner region, the small-x velocity solution is to zeroth order

$$u_0 = 1 \tag{38}$$

and, with this, there follows from equations (27) and (32)

$$h_\infty = 2x^{1/2}, \quad \tilde{T} = e^{-\tilde{y}^2/4x}/[2(\pi x)^{1/2}]. \tag{39}$$

For the outer region, that is, for the velocity, we proceed as follows: To first order, we assume a local similarity solution for the velocity difference $u - 1$, so that the stream function is given by

$$\psi = y + B(x)K(\zeta), \tag{40}$$

$$\zeta = y/x^{1/2}. \tag{41}$$

The requirements that the partial differential equation (34) reduces to an ordinary differential equation and that the boundary condition (37) be fulfilled yield $B = x$, so that the system of equations (33)–(35) and (37) becomes, to first order,

$$K''' + \tfrac{1}{2}\zeta K'' - \tfrac{1}{2}K' = 0, \tag{42}$$

$$K(0) = 0, \quad K''(0) = -\tfrac{1}{2}, \quad K'(\infty) = 0. \tag{43}$$

Solving for K', one obtains

$$K' = -\tfrac{1}{2}\zeta + \tfrac{1}{2}\zeta\,\mathrm{erf}(\zeta/2) + e^{-\zeta^2/4}/(\pi^{1/2}) \tag{44}$$

where the error function is defined as

$$\mathrm{erf}(\gamma) = (2/\pi^{1/2})\int_0^{\gamma} e^{-z^2}\,dz. \tag{45}$$

The velocity is then found from equation (40) to be

$$u = \partial\psi/\partial y = 1 + x^{1/2}K' \tag{46}$$

and, in particular, the centerline value is

$$u_0 = 1 + (x/\pi)^{1/2}. \tag{47}$$

We note that by taking the $Pr = \infty$ limit in Afzal's [4] results for small x, his zeroth order solution for the temperature reduces to the present solution (39), and his first order solution for the velocity reduces to that of equation (46). The foregoing solutions for small x are useful in giving the necessary starting values required by the numerical solution method to be described in Section 4.

Solutions appropriate for the case $x \to \infty$, that is, pure natural convection, have been obtained [5, 6]. Results which are relevant for comparison purposes are stated in the Appendix.

4. NUMERICAL METHOD

The boundary layer equations (8)–(10) were solved by using the well established Patankar–Spalding method [7]. This method utilizes the normalized von Mises variable; that is, instead of the y-coordinate, a non-dimensional stream-function coordinate is used

$$\omega = \bar{\psi}/\bar{\psi}_e, \quad \bar{\psi} = \int_0^{\bar{y}} \bar{u}\,d\bar{y} \tag{48}$$

where $\bar{\psi}_e$ denotes the value of $\bar{\psi}$ at the edge of the boundary layer. The finite difference grid then spans the range $x > 0$, $0 \leqslant \omega \leqslant 1$. In the x, ω variables, the system of equations (8)–(10) takes the form

$$\psi_e \frac{\partial \phi}{\partial x} - \omega \frac{d\psi_e}{dx} \frac{\partial \phi}{\partial \omega} = \frac{\partial}{\partial \omega}\left[\Gamma_\phi (u/\psi_e) \frac{\partial \phi}{\partial \omega}\right] + (\psi_e/u) S_\phi \tag{49}$$

where ϕ is either u or T, $\Gamma_u = 1$, $\Gamma_T = 1/Pr$, $S_u = T$, $S_T = 0$, and ψ_e is the dimensionless counterpart of $\bar{\psi}_e$. The finite difference scheme adopted in the Patankar–Spalding method is a fully implicit marching scheme whose accuracy is second order in ω (for grid Reynolds numbers less than about two) and first order in x.

The continuity equation has dropped out of the system, but instead, the unknown function $d\psi_e/dx$ has appeared. This function is a measure of the rate at which fluid is entrained into the plume, and it has to be determined as part of the solution by applying an additional constraint at the edge of the plume. Furthermore, the system of equations (8)–(10) has a singularity at $x = 0$, so that the integration has to be initiated at a very small value of x (x_i, say) with values of the dependent variables obtained from an analytical solution. For a further discussion on the determination of $d\psi_e/dx$ and initial values, see ref. [8].

Starting values at $x_i = 10^{-4}$ were obtained from equations (A1) and (A5) for $Pr = 0.72$ and 5, and from equation (46) for $Pr = \infty$. A uniform grid was used for ω, and the number of grid points for the range $0 \leqslant \omega \leqslant 1$ was 35. The local step length in x was determined by incrementing ψ_e by 1% of its value at the preceding step. This procedure gave rise to about 1500 points in the x-direction to cover the region of interest ($10^{-4} \leqslant x \leqslant 10^8$).

For $Pr = \infty$, there is a considerable simplification since only the equation for u, equation (34), has to be solved by the finite difference method. The boundary condition (37) is linearized to yield

$$(\partial u/\partial y)_0 = -1/u_{0p} + u_0/2u_{0p}^2 \tag{50}$$

where u_0 is the current (unknown) value of the centerline velocity and u_{0p} is the value at the preceding step. When u_0 at each x has been obtained, $h_\infty(x)$ was determined from equation (27) by trapezoidal rule integration and, with this, the temperature solution follows directly from equation (32).

5. RESULTS AND DISCUSSION

5.1. *Centerline velocity and temperature*

One of the main characteristic features of the plume is its centerline velocity. The variation of the centerline velocity as a function of the vertical coordinate is presented in Fig. 1. The ordinate variable is the dimensionless velocity $u_0 = \bar{u}_0/\bar{u}_\infty$, while $x^{1/4}$ is used on the abscissa in order to obtain a more compact presentation than would have occurred had x itself served as the abscissa variable. It may be noted that x not only measures the vertical distance above the line source, but it also serves as an index of the relative strengths of the forced and natural convection (i.e. $x = Gr^2/Re^5$). Thus, at small x ($Re^5 \gg Gr^2$), the mixed convection flow is dominated by forced convection, while natural convection plays the dominant role for large x ($Gr^2 \gg Re^5$).

The figure conveys the u_0 vs x distributions for Prandtl numbers of 0.72, 5, and ∞ (solid lines). Also appearing in the figure are dashed and dot–dashed lines which respectively represent the u_0 vs x distributions for pure natural convection and pure forced convection. These lines may be regarded as asymptotes for the mixed convection solutions. The forced convection line ($u_0 = 1$) is applicable for all Prandtl numbers, while the natural convection line that is shown in the figure corresponds to $Pr = \infty$. The natural convection lines for the other Prandtl numbers

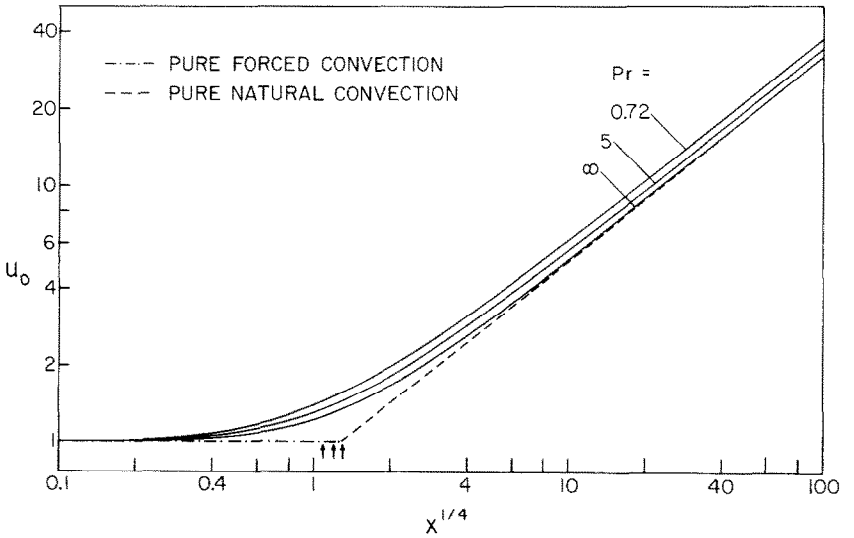

FIG. 1. Distribution of the plume centerline velocity.

have been omitted because their presence would have caused congestion and overlapping. It may be noted that since $u_0 \sim x^{1/5}$ for pure natural convection, then, for the natural convection asymptote, $u_0 \sim (x^{1/4})^{4/5}$.

The intersections of the forced and natural convection asymptotes have been identified by arrows positioned just below the abscissa axis. The rightmost arrow corresponds to the intersection for the $Pr = \infty$ case that can be seen in the figure, while the other arrows are for the $Pr = 5$ and 0.72 intersections (right to left) which are not shown in the figure.

Examination of Fig. 1 shows that the centerline velocity, initially equal to the forced convection value $u_0 = 1$, increases with increasing distance from the line source of heat. The increase is due to the action of buoyancy. Further study of the figure reveals that, in effect, the u_0 vs x distribution for the mixed convection problem 'rounds the corner' of the corresponding envelope curve made up of the pure forced and natural convection asymptotes. In general, the envelope curve tends to underestimate the centerline velocity. The greatest deviation between the actual mixed convection curve and the envelope curve occurs at the x value at which the latter experiences its change of slope (indicated by the arrows in Fig. 1). The values of $x^{1/4}$ at which these maximum deviations occur are 1.09, 1.20, and 1.30, respectively for $Pr = 0.72$, 5, and ∞. At these points, the respective envelope curves lie 31, 28, and 26% below the corresponding mixed convection curves.

It is also of interest to inquire about the distance from the line source at which the u_0 distribution from the mixed convection solution, in effect, coincides with that for pure natural convection. A 2% approach is adopted here as the criterion for the *de facto* coincidence of the two solutions. The x values at which the 2% approach is achieved are 5.8×10^3, 1.3×10^5, and 3.1×10^5, respectively for $Pr = 0.72$, 5, and ∞. Beyond these x values, u_0 values for the mixed convection problem can be obtained to high accuracy from the pure natural convection solution.

Attention is next turned to the variation of the centerline temperature of the plume as a function of the vertical distance from the line source, as presented in Fig. 2. As for the centerline velocity, results for the centerline temperature are given for $Pr = 0.72$, 5, and ∞. In addition, a complete envelope curve is shown for $Pr = 0.72$, and the natural convection asymptotes for $Pr = 5$ and ∞ are also included (complete envelope curves for these Prandtl numbers are not shown to preserve clarity). The break points in the envelope curves are indicated by arrows positioned at the top of the figure, respectively at $x^{1/4} = 3.13$, 1.94 and 1.37 for $Pr = 0.72$, 5 and ∞.

It should be noted that the ordinate variable includes certain powers of x and Pr in addition to the dimensionless centerline temperature T_0. The choice of this ordinate group is motivated by the fact that $T_0(x/Pr)^{1/2} = \text{constant} = 1/2\pi^{1/2}$ in the limit as $x \to 0$ (pure forced convection). Thus, with $T_0(x/Pr)^{1/2}$ as the ordinate, all of the mixed convection curves tend to a common horizontal line (independent of Prandtl number) for small x. Furthermore, in terms of this group, the natural convection asymptotes are of the form $T_0(x/Pr)^{1/2} \sim (x^{1/4})^{-4/10}$. It may also be useful to note that

$$T(x/Pr)^{1/2} = [(\bar{T} - \bar{T}_\infty)/\theta_T](Re/Pr)^{1/2}.$$

From Fig. 2, it can be seen that the centerline temperature decreases with increasing distance from the line source and that the decrease is more rapid as the plume progresses from forced convection dominance (small x) to natural convection dominance (large x). Also, the envelope curves tend to overestimate the centerline temperature compared with that given by the actual mixed convection solution, and this is just opposite to what was found for the centerline velocity. The greatest deviation between a mixed convection solution curve and its corresponding envelope curve occurs at the break point of the latter. For $Pr = 0.72$, 5, and ∞, the break-point values of the respective envelope curves are high by 24, 23, and 21%.

The approach of the centerline temperature for the mixed convection case to its natural convection asymptote occurs at smaller values of x as the Prandtl number increases, which is just opposite to the behavior of the centerline velocity. A 2% approach is achieved at $x = 7.4 \times 10^6$, 5.3×10^5, and 3.1×10^4, respectively for $Pr = 0.72$, 5, and ∞.

Before leaving this section, it is appropriate to compare the present u_0 and T_0 results with

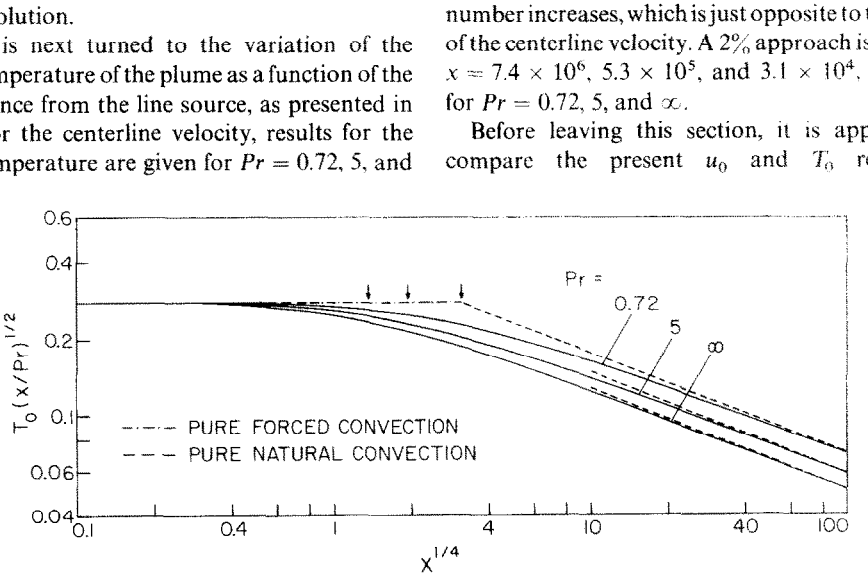

FIG. 2. Distribution of the plume centerline temperature.

corresponding results in the literature. As noted in the Introduction, Afzal [4] dealt with the case of $Pr = 0.72$. His graphical presentation for u_0 and T_0 could not be read with acceptable accuracy. Therefore, to enable a comparison, it was necessary to re-evaluate his series solution.

The comparison was made over the range from $x = 25$ to 10^8. The agreement of the u_0 results from the two solutions was found to be in the 0.3–0.4% range, with the T_0 agreement ranging from 0 to 0.6%. This level of agreement is an affirmation of both methods of solution.

Consideration will now be given to the development of an algebraic representation for the centerline velocity and temperature results. The objectives of this development are to provide results for all gas and liquid Prandtl numbers (rather than for only a few discrete values) and to express the x-dependence algebraically (rather than graphically). In this regard, it is believed that an algebraic representation offers greater convenience and accuracy for application than does a graphical representation.

To begin the development, it is useful to note that for pure forced convection and pure natural convection

$$u_0 = 1, \quad u_0 = x^{0.2}F'(0) \tag{51}$$

respectively. If $a \equiv 1$ and $b \equiv F'(0)$, then a u_0 representation which coincides with these small x and large x asymptotes can be written as

$$u_0 = [a^{1/n} + (bx^{0.2})^{1/n}]^n. \tag{52}$$

For each of the three investigated Prandtl numbers, the value of n was determined by equating the u_0 from equation (52) to the numerically determined value for the mixed convection plume, with the matching performed at x corresponding to the condition $a = bx^{0.2}$. The thus-determined n values are very well represented by

$$n = 0.53 - 0.09/Pr^{0.5}. \tag{53}$$

Equation (53) provides the ns needed in the evaluation of equation (52). Also, $a = 1$ for all Pr and $b = F'(0) = 0.810$, 0.860, and 0.934 for $Pr = 0.72$, 5, and ∞. Furthermore, an extensive tabulation of $F'(0)$ values is provided by Fujii [9].

To test the accuracy of equation (52), it was employed to evaluate u_0 over an extensive range of x for each of the three investigated Prandtl numbers. From this, it was found that the extreme error in the u_0 provided by equation (52) was about 3%, thereby affirming the utility of the algebraic representation.

A similar approach was employed for the centerline temperature distribution, yielding

$$T_0(x/Pr)^{1/2} = c/[1 + (cx^{0.1}/d)^{1/m}]^m \tag{54}$$

where

$$c = 0.282, \quad d = H(0)/Pr^{1/2}, \quad m = 0.26 + 0.04/Pr^{0.5} \tag{55}$$

and $d = 0.445$, 0.368 and 0.320 for $Pr = 0.72$, 5, and ∞, with a more extensive tabulation available in ref. [9]. The extreme error in the results provided by equation (54), as determined by comparisons with the actual mixed convection solutions, is about 2%. Thus, the algebraic representation for T_0 is highly accurate for all Prandtl numbers and x values.

5.2. *Plume width*

The width of the plume and its variation with vertical distance from the line source is another important result. Two widths may be considered, one for the velocity field and the other for the temperature field.

With respect to the velocity field, it should be noted that the presence of the line source creates a velocity distribution that is superposed atop the uniform forced convection approach flow $u = 1$. It is, therefore, appropriate to take account of this uniform 'background' velocity in defining the plume width. The definition to be employed here is that the plume width δ corresponds to the dimensionless distance from the axis where

$$(u-1)/(u_0-1) = 0.05. \tag{55}$$

Since u_0 varies with x, so also will δ. In actuality, since the plume is symmetric about the axis, δ is half the overall width of the plume.

The variation of δ with x is plotted in Fig. 3 for $Pr = 0.72$, 5, and ∞. The ordinate variable is $\delta/x^{1/2}$, where the factor $x^{1/2}$ is introduced because $\delta \sim x^{1/2}$ for small x. Also, in terms of dimensional

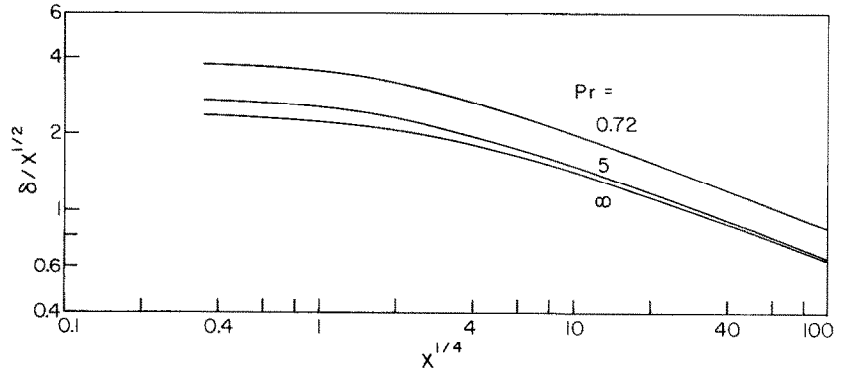

FIG. 3. Half-width of the plume velocity profile.

quantities, $\delta/x^{1/2} = (\bar{\delta}/\bar{x})Re^{1/2}$. As before, $x^{1/4}$ is used as the abscissa variable to obtain a compact presentation.

As expected, the plume width increases with x. The $x^{1/2}$ increase, which holds for small x, gives way to a somewhat slower increase at larger x. Thus, if x_2 and x_1 respectively correspond to $x = 10^8$ and 10^4, then $\delta_2/\delta_1 \sim 45$ while $(x_2/x_1)^{1/2} = 100$. At large x, it appears that δ takes on the x dependence predicted by the pure natural convection solution, i.e. $\delta/x^{1/2} \sim x^{-0.1}$. However, the numerical values of δ do not coincide with those for pure natural convection because the portion of the velocity profile that is adjacent to the lateral edge of the plume is influenced by the forced convection background velocity.

At any given x, the plume width decreases with increasing Prandtl number. The sensitivity of δ to Pr is small for intermediate and large Prandtl numbers (i.e. between 5 and ∞). Between $Pr = 0.72$ and 5, there is about a 25% decrease in δ.

At this point, it is appropriate briefly to discuss Afzal's results [4] for the plume width. His width δ^* was defined as

$$\bar{u}_\infty \bar{\delta}^* = \int_0^\infty (\bar{u} - \bar{u}_\infty)\, d\bar{y} \tag{56}$$

which resembles the displacement thickness of a boundary layer. The feature of equation (56) which appears to be inappropriate for the present problem is the use of $\bar{u}_\infty$ as the characteristic velocity of the plume (i.e. as the multiplier of $\bar{\delta}^*$). A more reasonable characteristic velocity would be $\bar{u}_0$. In view of this objection, it is not believed that the $\bar{\delta}^*$ results of Afzal (which correspond to his single Prandtl number of 0.72) are physically meaningful.

The thermal width δ_T of the plume will now be considered. It will be defined as the dimensionless distance from the plume axis where

$$T/T_0 = 0.05. \tag{57}$$

The δ_T values determined according to this definition are plotted in Fig. 4 in the form $\delta_T(Pr/x)^{1/2}$ vs $x^{1/4}$ where $\delta_T(Pr/x)^{1/2} = 3.46$ as $x \to 0$ for all Pr. Also, it may be noted that $\delta_T(Pr/x)^{1/2} = (\bar{\delta}_T/\bar{x})(RePr)^{1/2}$.

As was also true for δ, the thermal width δ_T increases at first as $x^{1/2}$, with a somewhat slower increase at larger x. In addition, the thermal width decreases with the Prandtl number, the decrease going as $Pr^{1/2}$ at small x and slightly more rapidly at larger x. From a comparison of Figs. 3 and 4, it is seen that $\delta_T \simeq \delta$ for $Pr = 0.72$, but that $\delta_T < \delta$ for higher Prandtl numbers. At large Prandtl numbers, the thermal width of the plume is much smaller than the velocity width.

5.3. *Velocity and temperature profiles*

The evolution of the velocity profile in the plume with increasing vertical distance from the line source is illustrated in Fig. 5. The figure is a composite of four graphs, each of which corresponds to a specific value of x, namely, $x = 10^2$, 10^4, 5×10^5, and 10^7. In each graph, the dimensionless velocity $u(= \bar{u}/\bar{u}_\infty)$ is plotted as a function of $y/x^{1/2} = (\bar{y}/\bar{x})Re^{1/2}$. Of particular note is that the range of the ordinate has been approximately doubled from graph to graph in order to accommodate the increase in velocity that accompanies an increase in the vertical distance from the line source. The abscissa range has been maintained the same in all graphs by inclusion of the factor $1/x^{1/2}$ in the abscissa variable.

The velocity profiles for the various Prandtl numbers display characteristic shapes. For all cases, the maximum velocity is attained at the axis ($y = 0$) and, as y increases, the velocity decreases toward $u = 1$. For $Pr < \infty$, the velocity profile is flat (i.e. $\partial u/\partial y = 0$) at the axis, but it is evident by comparing the curves for $Pr = 0.72$ and 5 that the extent of the flat region diminishes with increasing Prandtl number. For the $Pr = \infty$ case, $\partial u/\partial y \neq 0$ at $y = 0$ [see equation (37)]. As a consequence of this, the inflection point that appears in the curves for $Pr < \infty$ disappears when $Pr = \infty$.

Away from the immediate neighborhood of the axis, the curves are ordered from upper to lower with increasing Prandtl number. However, owing to the aforementioned tendency toward greater near-axis flattening at lower Prandtl numbers, the ordering of the curves is reversed at and near the axis.

As implied by the change in the ordinate range, there is a significant increase in the velocity magnitude with x, reflecting the role of the buoyancy. There is also a

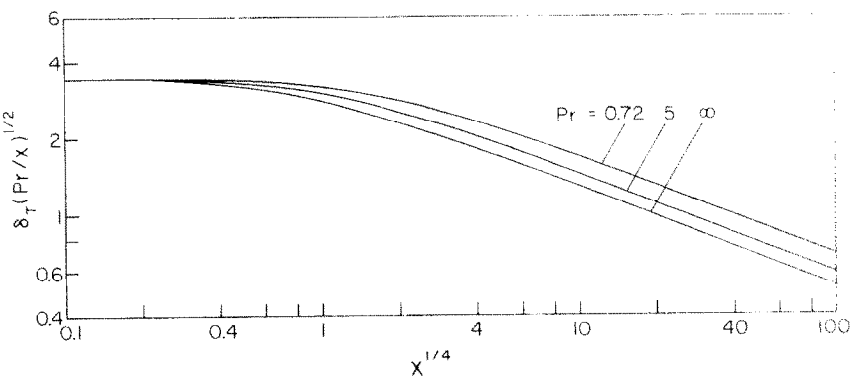

FIG. 4. Half-width of the plume temperature profile.

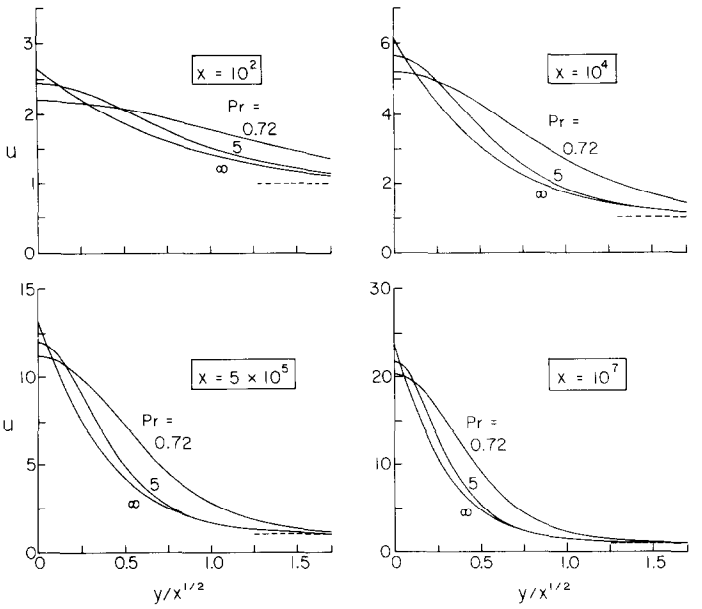

FIG. 5. Plume velocity profiles.

change in the shape of the curves. Those for small x tend to be relatively flat, while for larger x the curves are more peaked.

Some consideration was given to an alternative presentation in which u/u_0 was the ordinate variable. Owing to the just-mentioned change in shape of the curves, the u/u_0 representation did little to unify the results and, therefore, was not used.

The situation is quite different for the temperature profiles, as witnessed by Fig. 6. Here, by plotting T/T_0 vs y/δ_T, a profile representation was obtained that is nearly independent of both x and Pr. The virtual x-independence of the normalized profiles is illustrated in the upper part of Fig. 6 for $Pr = 0.72$, but a similar finding pertains to the other Prandtl numbers. In fact, the curves are even closer together for $Pr = 5$ and collapse to a single curve for $Pr = \infty$. Furthermore, in the lower part of Fig. 6, the curves for a fixed x are seen to show only slight dependence on the Prandtl number. It was verified that a similar Prandtl number dependence occurs at all x.

The temperature profiles were able to be correlated because they all have common shapes. In particular, all attain a flat maximum ($\partial T/\partial y = 0$) at $y = 0$, display an off-axis inflection, and go to zero at large y. These characteristics were not possessed by all the velocity profiles, with the result that they could not be successfully correlated, as were the temperature profiles.

6. CONCLUDING REMARKS

Both numerical and analytical methods have been employed to determine the velocity and temperature fields in the mixed convection plume above a horizontal line source of heat situated in a uniform, vertical forced

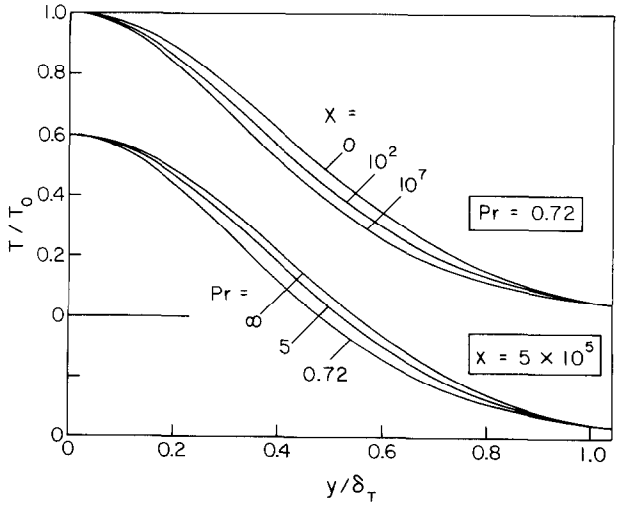

FIG. 6. Plume temperature profiles.

convection approach flow. The sequence of the work was first to obtain solutions for several specific Prandtl numbers in the range $0.72 \leqslant Pr \leqslant \infty$ and then to generalize the results for certain key quantities to make them applicable to all Prandtl numbers in this range, as well as for all vertical distances above the line source.

In general, at relatively small distances above the source, the forced convection nature of the approach flow plays a dominant role. At larger distances, however, buoyancy asserts itself more and more strongly and, at sufficiently large distances, the plume resembles that for pure natural convection.

In presenting the results for the centerline velocity and temperature of the mixed convection plume as a function of the distance from the line source, the forced convection and natural convection asymptotes were employed to construct an envelope curve for the corresponding mixed convection curve. For the centerline velocity, the envelope curve bounds the mixed convection curve from below, with a maximum deviation of about 30%. On the other hand, the envelope curve for the centerline temperature falls above the mixed convection curve by, at most, 25%. The distance above the line source at which the mixed convection plume approaches to within a fixed tolerance (e.g. 2%) of the natural convection plume has been identified and is given in the paper for the various Prandtl numbers.

Generalization of the results for the centerline velocity and temperature to apply to all Prandtl numbers and distances from the line source is respectively accomplished by equations (52) and (53) and by equations (54) and (55). These algebraic equations were found to be accurate to better than 3% for the velocity and 2% for the temperature.

The width of the plume was defined in terms of the distance from the axis at which the velocity and temperature had declined to 5% of the centerline-to-ambient difference. Both the velocity and thermal widths, δ and δ_T, respectively, increased with distance from the line source, but at a slower rate at larger distances. For high Prandtl numbers, $\delta_T \ll \delta$.

The velocity profiles were quite flat for small distances above the line source and became more peaked at greater distances. The high-Pr profiles were of a somewhat different character than those for the other Prandtl numbers. On the other hand, the temperature profiles were generally bell-shaped at all vertical distances and Prandtl numbers.

REFERENCES

1. W. W. Wood, Free and forced convection from fine hot wires, *J. Fluid Mech.* **55,** 419–438 (1972).
2. P. Wesseling, An asymptotic solution for slightly buoyant plume, *J. Fluid Mech.* **70,** 81–87 (1974).
3. S. Nakai and T. Okazaki, Heat transfer from a horizontal circular wire at small Reynolds and Grashof numbers—II, *Int. J. Heat Mass Transfer* **18,** 397–413 (1975).
4. N. Afzal, Mixed convection in a two-dimensional buoyant plume, *J. Fluid Mech.* **105,** 347–368 (1981).
5. D. B. Spalding and R. G. Cruddace, Theory of the steady laminar buoyant flow above a line heat source in a fluid of large Prandtl number and temperature-dependent viscosity, *Int. J. Heat Mass Transfer* **3,** 55–59 (1961).
6. H. K. Kuiken and Z. Rotem, Asymptotic solution for plume at very large and small Prandtl numbers, *J. Fluid Mech.* **45,** 585–600 (1971).
7. D. B. Spalding, GENMIX: *A General Computer Program for Two-Dimensional Parabolic Phenomena.* Pergamon Press, Oxford (1977).
8. S. E. Haaland, A note on the calculation of the entrainment rate and initial values for the Patankar–Spalding method. submitted for publication.
9. T. Fujii, I. Morioka and H. Uehara, Buoyant plume above a horizontal line heat source, *Int. J. Heat Mass Transfer* **16,** 755–768 (1973).

APPENDIX

SOLUTIONS FOR VERY SMALL AND VERY LARGE x

When x is close to zero, we have the pure forced convection case where

$$u = 1, \quad v = 0 \tag{A1}$$

so that the temperature equation (10) reduces to the simple heat equation

$$\frac{\partial T}{\partial x} = (1/Pr)\frac{\partial^2 T}{\partial y^2} \tag{A2}$$

with the conditions

$$\partial T/\partial y(0) = T(\infty) = 0, \tag{A3}$$

$$\tfrac{1}{2} = \int_0^\infty uT \, dy. \tag{A4}$$

A similarity solution of this system is found, in a straightforward manner [1], to be in our variables

$$T = (Pr/4\pi x)^{1/2} \exp(-y^2 Pr/4x). \tag{A5}$$

For very large x, $\bar{u}_0 \to \infty$, so that $\bar{u}_\infty/\bar{u}_0 \to 0$. Hence, the appropriate boundary condition for the velocity at infinity now becomes $u(\infty) = 0$. This problem, therefore, reduces to the pure natural convection case for which the most complete and accurate solutions can be found in Fujii *et al.* [9]. Similarity solutions for this problem are obtained using the following transformation of variables

$$\bar{u} = (\nu G^2)^{1/5} \bar{x}^{1/5} F'(\eta), \tag{A6}$$

$$\bar{T} - \bar{T}_\infty = \theta_T (\nu^2/G)^{1/5} \bar{x}^{-3/5} H(\eta), \tag{A7}$$

$$\eta = \bar{y}/h, \quad h = (\nu^2/G)^{1/5} \bar{x}^{2/5} \tag{A8}$$

where G is a "reduced" gravitational acceleration given by

$$G = g\beta\theta_T = g\beta Q/\rho c_p \nu. \tag{A9}$$

The functions F' and H are found from the solution of the following system of ordinary differential equations:

$$F''' + (3/5)FF'' - (1/5)F'^2 + H = 0, \tag{A10}$$

$$H' + (3/5)PrFH = 0, \tag{A11}$$

$$F = F'' = 0 \quad \text{at} \quad \eta = 0, \tag{A12}$$

$$F' = H = 0 \quad \text{at} \quad \eta = \infty, \tag{A13}$$

$$\tfrac{1}{2} = \int_0^\infty F'H \, d\eta \tag{A14}$$

in which the Prandtl number appears as a parameter. In this system, an integration has been performed to obtain equation (A11) in contrast to the corresponding unintegrated equation

of Fujii *et al.* [9], and a boundary condition $H'(0) = 0$, which now is seen to be automatically satisfied because $F(0) = 0$, has been dropped.

When $Pr \to \infty$, we have the lowest order (i.e. order Pr) from [6]

$$H = (3Pr/10\pi a_0)^{1/2} \exp[(-3a_0 Pr/10)\eta^2]$$

where $a_0 = F'(0)$. In terms of the non-dimensional variables defined by equations (7) and (A7), this becomes

$$Tx^{3/5}Pr^{-1/2} = (3/10\pi a_0)^{1/2} \exp[(-3a_0 Pr/10)y^2/x^{4/5}]. \tag{A15}$$

The non-dimensional stream function $F(\eta)$ is now found from

$$F''' + (3/5)FF'' - (1/5)F'^2 = 0,$$
$$F(0) = 0, \quad F''(0) = -1/[2F'(0)], \quad F'(\infty) = 0. \tag{A16}$$

The numerical solution of equations (A16) gives, in particular, $a_0 = F'(0) = 0.9336$.

It is of interest to show that equation (A15) can be obtained from the solution given in Section 3. First, we note that the centerline velocity in the non-dimensional variables defined by equation (7) is

$$u_0 = a_0 x^{1/5}. \tag{A17}$$

Substitution of equation (A17) into equation (27) gives

$$h_\infty = (10/3a_0)^{1/2} x^{2/5}. \tag{A18}$$

Then, by substitution of equations (15), (A17), and (A18) into equation (32), equation (A15) emerges. However, equation (A15) can only be an asymptote to the mixed convection problem because equation (A17) is only valid for very large x, so that equation (A18), which was obtained by integration of the velocity from *zero* to x, might not be too accurate for other than very large x.

The above solutions for extreme values of x give asymptotes for the mixed convection problem. We have for the centerline values

$x \to 0$

$$u_0 = 1, \tag{A19}$$

$$T_0(x/Pr)^{1/2} = (1/4\pi)^{1/2}, \tag{A20}$$

$x \to \infty$

$$u_0 = x^{1/5}F'(0), \tag{A21}$$

$$T_0(x/Pr)^{1/2} = x^{-1/10}H(0)/Pr^{1/2} \tag{A22}$$

where the necessary constants are given in Table 1.

Table 1. Constants for equations (A21) and (A22)

	Pr		
	0.72	5	∞
$F'(0)$	0.8096	0.8597	0.9336
$H(0)/Pr^{1/2}$	0.4447	0.3679	0.3198

PANACHE DE CONVECTION MIXTE AU DESSUS D'UNE SOURCE LINEAIRE HORIZONTALE SITUEE DANS UN ECOULEMENT FORCE

Résumé—On utilise des techniques analytiques et numériques pour résoudre les champs de vitesse et de température dans un panache bidimensionnel de convection mixte, pour un nombre de Prandtl variant de 0,72 jusqu'à l'infini. La méthode de développement interne et externe est utilisée pour le cas $Pr = \infty$, tandis que la méthode parabolique, aux différences finies, fournit les solutions pour les autres nombres de Prandtl. En général, le panache se déploie, quand augmente la distance à la source linéaire, depuis la convection forcée jusqu'à ce qui ressemble à la convection naturelle pure. Les variations de vitesse et de température sur la ligne des centres avec la distance à la source sont bordées par des courbes enveloppes construites à partir des asymptotes pour la convection forcée pure et la convection naturelle. Des relations algébraiques très précises, valables pour tous les nombres de Prandtl et toutes les distances, sont développées pour généraliser les résultats obtenus pour les nombres de Prandtl discrets. La largeur du panache augmente avec la distance à la source, mais d'autant moins vite que la distance augmente. Les formes des profils de vitesse changent avec la distance et le nombre de Prandtl, tandis que tous les profils de température possède la forme commune en cloche.

DIE AUFTRIEBSTRÖMUNG BEI GEMISCHTER KONVEKTION ÜBER EINER WAAGERECHTEN LINIENQUELLE BEI ANSTRÖMUNG DURCH ERZWUNGENE KONVEKTION

Zusammenfassung—Es wurden sowohl analytische als auch numerische Verfahren angewendet, um Geschwindigkeits- und Temperaturfelder der zweidimensionalen gemischten Auftriebsströmung für Prandtl-Zahlen von 0,72 bis unendlich zu berechnen. Für den Fall $Pr = \infty$ wurde die Methode der inneren und äußeren Reihenentwicklung angewendet, während für die anderen Prandtl-Zahlen ein parabolisches finites Differenzenverfahren die Lösungen lieferte. Prinzipiell wurde festgestellt, daß sich die Auftriebsströmung mit zunehmender Entfernung von der Linienquelle in ihrem Charakter von der für erzwungene Konvektion typischen Form zu einer Form hin entwickelt, die bei reiner freier Konvektion auftritt. Die Änderungen von Geschwindigkeit und Temperatur an der zentralen Achse mit der Entfernung von der Linienquelle wurden durch Hüllkurven eingegrenzt, die aus den Asymptoten für reine erzwungene und reine freie Konvektion konstruiert wurden. Äußerst genaue algebraische Gleichungen für alle Prandtl-Zahlen und alle Entfernungen von der Linienquelle wurden hergeleitet, um die Ergebnisse, die für die verschiedenen diskreten Prandtl-Zahlen erhalten worden waren, zu verallgemeinern. Die Breite des Auftriebsgebietes vergrößerte sich mit dem Abstand von der Quelle, jedoch mit zunehmender Entfernung langsamer. Die Gestalt der Geschwindigkeitsprofile änderte sich sowohl mit der Entfernung als auch mit der Prandtl-Zahl, die Temperaturprofile zeigten dagegen alle eine gemeinsame glockenartige Form.

СМЕШАННАЯ КОНВЕКЦИЯ В ПОДЪЕМНОМ ТЕЧЕНИИ НАД ГОРИЗОНТАЛЬНЫМ ЛИНЕЙНЫМ ИСТОЧНИКОМ, ОБТЕКАЕМЫМ НАБЕГАЮЩИМ ПОТОКОМ С ВЫНУЖДЕННОЙ КОНВЕКЦИЕЙ

Аннотация — Аналитическими и численными методами получены решения для полей скорости и температуры в двумерной струе в режиме смешанной конвекции в диапазоне изменения чисел Прандтля от 0,72 до бесконечности. Для случая $Pr = \infty$ использовался метод внутренних и внешних разложений, а для других значений числа Прандтля — параболический метод конечных разностей. В целом найдено, что по мере удаления от линейного источника характер струи изменяется от режима течения чисто вынужденной конвекции до режима естественной конвекции. Изменения скорости и температуры вдоль оси подъемной струи по мере удаления от линейного источника описываются кривыми, построенными по асимптотам для чисто вынужденной и чисто естественной конвекции. С целью обобщения результатов, полученных для различных дискретных значений числа Прандтля, получены весьма точные алгебраические соотношения, справедливые для всех чисел Прандтля и всех расстояний от линейного источника. Ширина подъемной струи увеличивается с расстоянием от источника, причем тем медленнее, чем дальше от него. Вид профилей скорости изменяется в зависимости как от расстояния, так и от числа Прандтля, в то время как профили температур имеют обычную колоколобразную форму.